Photoionization Study of Fe(CO)$_5$ and Ni(CO)$_4$

G. Distefano*

Institute for Materials Research, National Bureau of Standards, Washington, D.C. 20234

(December 5, 1969)

Photoionization yield curves from onset to 600Å, and ionization threshold values have been obtained for the ions Fe(CO)$_5^+$, Fe(CO)$_4^+$, Fe(CO)$_3^+$, Fe(CO)$_2^+$, Fe(CO)$^+$, Fe$^+$ and CO$^+$ from iron pentacarbonyl, and for Ni(CO)$_4^+$, Ni(CO)$_3^+$, Ni(CO)$_2^+$, Ni(CO)$^+$, Ni$^+$, and CO$^+$ from nickel tetracarbonyl. From these curves, information on the ionization-fragmentation processes of Fe(CO)$_5$ and Ni(CO)$_4$ under photon impact, have been obtained. Differences in the threshold energies as determined by photon and by electron impact methods increase with the fragmentation. The appearance potentials and the heats of formation of the metal-ions, agree within 0.1 eV, with those calculated from thermochemical data. The average bond dissociation energy of the neutral molecule agrees within 0.02 eV, with the thermochemical values. The kinetic shift for the formation of Fe$^+$ and Ni$^+$ ions is very small. The Ni$^+$ ion is most likely formed directly from the molecule ion rather than by a cascade fragmentation process.

Key words: Dissociation energies; Fe(CO)$_5$; heats of formation; ionization; mass spectrometry; Ni(CO)$_4$; vacuum ultraviolet spectroscopy.

1. Introduction

In recent years, the mass spectrometric study by electron impact of transition-metal carbonyls has received increasing attention [1, 2].[1] Although the data obtained in the same laboratory are well correlated [3, 4], they often differ from those obtained in other laboratories on the same molecules. Several reports are available on mass spectra and appearance potentials of the iron pentacarbonyl and nickel tetracarbonyl by electron impact [5 to 9] and one by photon impact without mass analysis [10] which determined the ionization potentials only. The agreement among the fragmentation patterns is satisfactory, considering that the spectra were obtained with different instruments, and under different experimental conditions such as electron energy and ion source temperature. However, the appearance potentials differ by as much as 1 eV or more especially for ions of low mass. Thus, the purpose of this work is to obtain more accurate values for the ionization thresholds for molecular and fragment ions, more reliable data for ion heats of formation, and bond dissociation energies in both the molecules and in the ions, and information on the ionization fragmentation processes under photon impact.

2. Experimental Procedure

Photoionization efficiency curves were obtained by means of the combined vacuum ultraviolet mono- chromator and mass spectrometer described in detail by Dibeler et al. [11, 12]. Data were obtained with an optical resolution of about 1Å, with an uncertainty in the absolute wavelength of 1Å or less over all wavelengths. The uncertainty in the reported relative ionization efficiency (ions per photon transmitted through the ion source) is of the order of 3 to 5 percent. It is ascribed principally to the uncertainty in measuring the number of electrons photoejected from a tungsten photon detector. At wavelength longer than 1200Å, we do not have a correction for the change of the quantum yield of the tungsten detector with the wavelength. All the data of figures 1 and 3 must be multiplied by a slowly decreasing factor going to longer wavelength. For this reason, the uncorrected part of the photoionization efficiency curves are plotted in different figures. The onset regions of the Fe(CO)$_5^+$, Ni(CO)$_4^+$ and Ni(CO)$_3^+$ ions have been repeated with a sodium salicylate detector with only minor differences noted. The samples were obtained from a commercial supplier. Mass spectrometric analysis showed no detectable impurities other than carbon monoxide. The following conversion factors were used throughout this paper.

$$1 \text{ eV molecule}^{-1} = 8065.73 \text{ cm}^{-1}$$
$$= 23.0609 \text{ kcal mol}^{-1}$$
$$1 \text{ kcal mol}^{-1} = 4.1840 \text{ kJ mol}^{-1}$$

3. Results and Discussion

Table 1 lists the relative abundances of the positive ions observed in the mass spectra of Fe(CO)$_5$ and

---

TABLE 1.   *Relative intensity of the ions in* $Fe(CO)_5$ *and* $Ni(CO)_4$ *mass spectra*

	Ref. [5] [a]	Ref. [6]	Ref. [7]	Ref. [8] [b]	Ref. [9]	This work
Energy in eV.	~ 25	30	50	50	70	21.22
Source temperature	Room temperature	250 °C	205 °C	150 °C	Room temperature	Room temperature
$Fe(CO)_5$						
$Fe(CO)_5^+$	30	25	18	43		10.3
$Fe(CO)_4^+$	24	35	22	50		11.6
$Fe(CO)_3^+$	12	18	11	22		2.2
$Fe(CO)_2^+$	95	30	24	36		18.8
$FeCO^+$	100	100	82	100		100.0
Fe^+	30	60	100	93		38.3
CO^+		10		"large"		1.8
$Ni(CO)_4$						
$Ni(CO)_4^+$	37		26	51	31.0	10.8
$Ni(CO)_3^+$	63		53	100	43.8	19.1
$Ni(CO)_2^+$	67		44	49	42.2	31.4
$Ni(CO)^+$	100		100	54	100.0	100.0
Ni^+	27		66	46	58.3	35.1
CO^+				"large"		21.3

[a] Derived from figure 2 of Ref. [5].

[b] Derived from figure 2 of Ref. [8].

$Ni(CO)_4$ at 21.22 eV (584Å). No metastable ions, double charged ions, or ions resulting from the rupture of the C—O bond were observed. The appearance potential of the CO^+ ion from these carbonyls is 14.01 ± 0.02 eV (885 ± 1Å). The threshold value and the shape of the curve (from the onset to 800Å) are exactly the same for those of CO^+/CO. Thus, the CO^+ ion is not formed by photon impact on the metal-carbonyls, but from molecular CO already present in the samples or formed by decomposition in the inlet system.

Comparing the relative abundances of table 1 with those previously reported [5, 9], we observe a smaller relative abundance for the ions of heavier mass. The apparent origin of the CO^+ and the relatively low intensity of the higher mass ions suggests that interpretation of results may be ambiguous due to decomposition [13, 14]. However, the threshold values of $Fe(CO)_4^+$, $Ni(CO)_3^+$, Fe^+ and Ni^+ ions show that these ions come from the molecular ion, and not from intermediate radicals. Therefore decomposition is not considered to have an important effect on the results. The differences between the present relative ion intensities and those previously reported can be ascribed to differences in source and inlet systems temperature [7], to the ionization beam, to its energy, to different apparatus and detectors.

$Fe(CO)_5^+$. Typical photoionization yield curves for the $Fe(CO)_5^+$ ion are shown in figures 1 and 2. The curve exhibits a weak onset at 1554 ± 1Å (7.98 ± 0.01 eV). Due to the size of the molecule, to its large number of electrons, and to the fact that the electron removed in the first ionization is a nonbonding or weakly bonding one (see later), the geometry of the ion is expected to remain the same as that of the molecule in its ground state. For these reasons the molecule ion is likely formed by $0'-0''$ (or $1'-1''$, etc.) transitions and no hot bands are expected on the low energy side of the threshold.

The threshold energy is lower than all electron impact data [5, 9], but it is very close to a previous photoionization value (7.95 eV) [10]. Taking the present threshold value as the heat of reaction, $\Delta H_0 = 184.0$ kcal mol^{-1} for $Fe(CO)_5 + h\nu \rightarrow Fe(CO)_5^+ + e$, and adding the heat of formation of the molecule [15],

$$\Delta Hf°[Fe(CO)_5] = -175.4 \text{ kcal mol}^{-1},$$

the heat of formation of the ion, $\Delta Hf°[Fe(CO)_5^+] = 8.6$ kcal mol^{-1} is obtained. This and the following thermodynamic values and threshold energies are summarized in table 2. This table also includes the lowest and highest threshold values obtained by electron impact. It is important to note that the appearance potentials for the M^+ and MCO^+ ions as measured by electron impact may differ by as much as 2 eV.
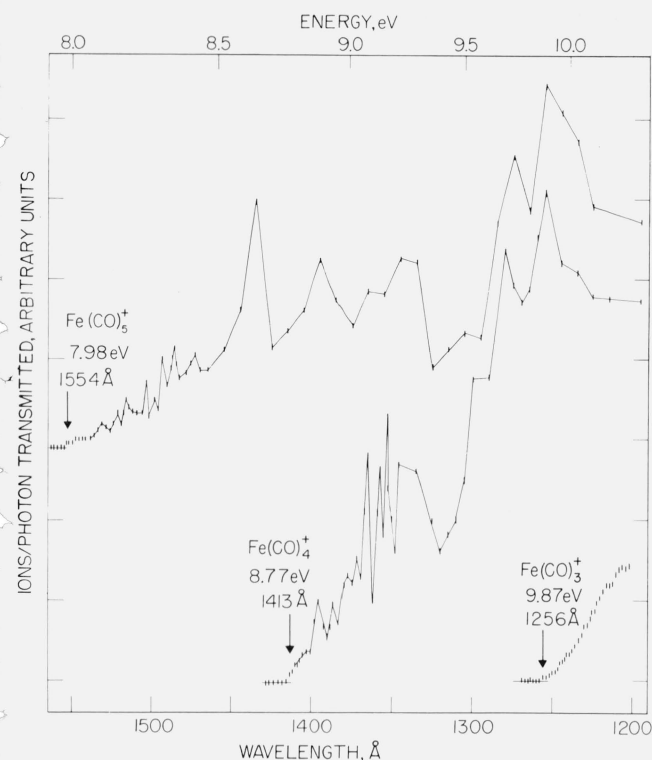
FIGURE 1. *Photoionization-yield curves from onset to 1200Å for* $Fe(CO)_5^+$, $Fe(CO)_4^+$, *and* $Fe(CO)_3^+$ *ions of iron pentacarbonyl.*
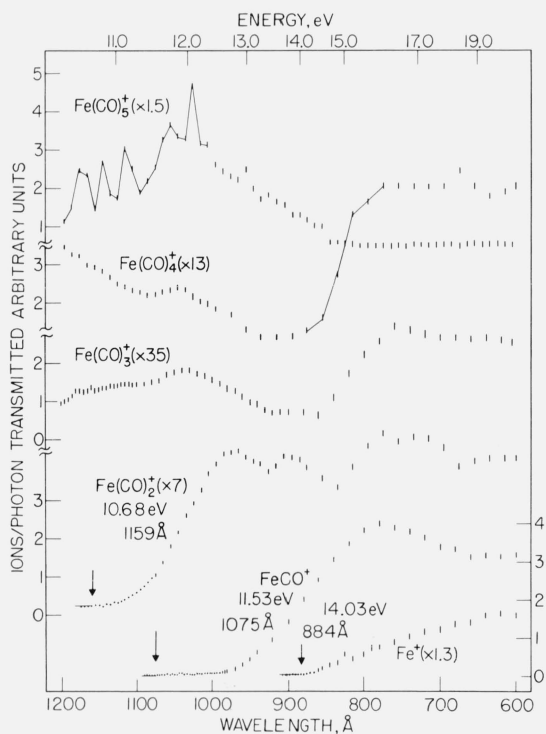

FIGURE 2. *Photoionization-yield curves from 1200 to 600Å for molecule and fragment ions of iron pentacarbonyl.*

The curve shows many autoionizing Rydberg levels from the onset to 855Å (14.50 eV) at which energy they appear to converge. The shape of the curve between 1000 and 855Å suggests that there is a slow decrease in excitation of more highly excited states of $Fe(CO)_5^+$. Where these peaks disappear, the molecule ion decomposes to form the excited $Fe(CO)_4^+$ fragment ion. At this energy the $Fe(CO)_4^+$ curve (see below) shows a new, abrupt and intense onset, which can be ascribed to a second ionization threshold. From 850 to 600Å, the molecule ion curve is very constant.

$Fe(CO)_4^+$. The $Fe(CO)_4^+$ ion shows (see figs. 1 and 2) a weak onset at 1413 ± 1Å (8.77 eV). The previous values [5, 9] range between 8.4 and 9.2 eV. Pignataro and Lossing [13] assigned the lower value to the direct ionization of the $Fe(CO)_4$ radical produced by thermal decomposition, whereas, the electron impact value of 9.1 eV was ascribed to the process

$$Fe(CO)_5 + e \rightarrow Fe(CO)_4^+ + CO + 2e.$$
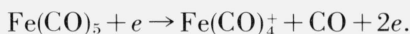
The present value can be taken as the heat of reaction, $\Delta H_0 = 202.2$ kcal mol^{-1} for

$$Fe(CO)_5 + h\nu \rightarrow Fe(CO)_4^+ + CO + e.$$

Using the heats of formation for $Fe(CO)_5$ and CO (-26.416 kcal mol^{-1}) [16], the value

$$\Delta Hf°[Fe(CO)_4^+] = 53.2 \pm 2 \text{ kcal mol}^{-1}$$

is obtained. From the onset to 1200Å the curve shows considerable structure due to autoionization. This is clearly correlated with the structure in the molecule ion curve, suggesting that the same processes are producing excited $Fe(CO)_5^+$ and $Fe(CO)_4^+$ ions. A similar process is observed in the $Ni(CO)_4$. From about 1200Å the $Fe(CO)_4^+$ ion curve is no longer parallel to the molecular ion curve and its intensity slowly diminishes until it exhibits a new onset at 855Å as discussed above.

$Fe(CO)_3^+$. The $Fe(CO)_3^+$ ion curve starts (see figs. 1 and 2) with a very weak steplike onset at 1256 ± 1Å (or 9.87 eV). This is a few tenths of an eV lower than the energy at which the $Fe(CO)_4^+$ ion curve begins to go down away from the molecule ion curve. From 1040 to 600Å the $Fe(CO)_3^+$ and $Fe(CO)_4^+$ ion curves are very similar. Likely the $Fe(CO)_3^+$ ion is coming from $Fe(CO)_4^+$ ion by a cascade process. The heat of formation,

$$\Delta Hf°[Fe(CO)_3^+] = 105 \pm 2 \text{ kcal mol}^{-1},$$

is obtained from the threshold value.

The initial part of the curve exhibits a number of steplike features at an average interval of 426 cm^{-1}. This value may be compared with the Fe-CO stretching frequency ν_{13} in the neutral molecule of 431 cm^{-1} [17]. This initial part of the curve does not have the same shape as the curve for the distribution of the thermal energy of the neutral molecule.

$Fe(CO)_2^+$. The $Fe(CO)_2^+$ ion curve starts at 1159 ± 1Å (10.68 eV) (see fig. 2). The onset region shows a tail on the low energy side with superimposed unresolved

	Photoionization threshold (eV)[a]	Electron impact threshold (eV)[b]	$\Delta Hf°$[c]	
$Fe(CO)_5$			*eV*	*kcal mol^{-1}*
$Fe(CO)_5^+$	7.98 ± 0.01	8.14 − 8.53	0.37 ± 0.02	8.6 ± 0.5
$Fe(CO)_4^+$	8.77 ± 0.1	8.34 − 10.0	2.31 ± 0.1	53.2 ± 2
$Fe(CO)_3^+$	9.87 ± 0.1	9.89 − 10.3	4.55 ± 0.1	105 ± 2
$Fe(CO)_2^+$	10.68 ± 0.1	10.92 − 11.8	6.51 ± 0.1	150.1 ± 2
$FeCO^+$	11.53 ± 0.1	12.9 − 14.0	8.51 ± 0.1	196.2 ± 2
Fe^+	14.03 ± 0.1	14.7 − 16.1	12.35 ± 0.1	284.7 ± 2
			[d] 12.28	[d] 283.16
$Ni(CO)_4$				
$Ni(CO)_4^+$	8.32 ± 0.01	8.35 − 8.75	2.07 ± 0.02	47.8 ± 0.5
$Ni(CO)_3^+$	8.77 ± 0.02	8.89 − 9.36	3.58 ± 0.02	82.6 ± 0.5
$Ni(CO)_2^+$	10.10 ± 0.1	10.21 − 10.7	6.14 ± 0.1	141.7 ± 2
$NiCO^+$	11.65 ± 0.1	12.17 − 13.5	8.84 ± 0.1	203.8 ± 2
Ni^+	13.75 ± 0.1	14.45 − 16.0	12.09 ± 0.1	278.7 ± 2
			[d] 12.15	[d] 280.24

[a] See text for discussion of estimated uncertainty in threshold values. Only Fe^+ and Ni^+ ions threshold have been corrected for the thermal energy the neutral molecules possess.
[b] Total range of reported electron impact values, (Refs. [5] through [9]).
[c] The assumed processes are $M(CO)_x + h\nu \rightarrow [M(CO)_{x-n}]^+ + nCO$.
[d] Calculated value from heat of formation and ionization potential of the metal atom [19, 20].

autoionization peaks, followed by steplike features at an average interval of 461 cm^{-1}. This value is to be compared with the Fe-CO stretching frequency ν_8 in the neutral molecule of 474 cm^{-1} [17]. These steplike features are a peculiarity of $Fe(CO)_3^+$ and $Fe(CO)_2^+$ ion curves. All other curves, both for iron and nickel carbonyls, show either autoionization peaks or a smooth continuum. Perhaps autoionization does not occur because the competing process of predissociation is much more probable. A similar effect has been reported for NH_3^+ molecule ion [18]. The remainder of the curve has maxima at about 960, 900, and 750Å. From 960 to 600Å the curve is very similar to that of the $Fe(CO)_3^+$ ion, again suggesting the production of the $Fe(CO)_n^+$ ions from the $Fe(CO)_{n+1}^+$ ions. From the threshold value, the $\Delta Hf°[Fe(CO)_2^+]$ is 150.1 ± 2 kcal mol^{-1}.

FeCO$^+$. The FeCO$^+$ ion curve starts with a weak, very long tail (see fig. 2) at 1075 ± 1Å (11.53 eV). From the threshold value, $\Delta Hf°(FeCO^+)$ is 196.2 ± 2 kcal mol^{-1}. The ion yield curve rises quickly starting at about 980Å and peaks at 780Å.

Fe$^+$. The Fe$^+$ ion curve also starts with a weak very long tail (see fig. 2). The onset is at 884 ± 2Å (14.03 eV), which might become 14.23 eV if the thermal energy of the molecule at 298 K (0.2 eV as calculated from ir frequencies [17]) is taken into account. From this value $\Delta Hf°(Fe^+) = 284.7$ kcal mol^{-1} is obtained. By using heat of formation ($\Delta Hf°(Fe) = 99.5$ kcal mol^{-1} [19],

$$\Delta Hf_0°Fe(CO)_5 = -175.8 \text{ kcal mol}^{-1} \text{ [15]},$$

$\Delta Hf_0°CO = -27.199$ kcal mol^{-1} [16]) and I(Fe) = 7.87 eV [20] to calculate the theoretical threshold of the

process $Fe(CO)_5 + h\nu \rightarrow Fe^+ + 5\ CO + e$, 13.92 eV is obtained if the quantities involved are considered at 0 K, and 14.16 eV at room temperature. Thus, the results agree with thermochemical values to within about 0.1 to 0.3 eV.

A calculation based on the Quasi Equilibrium Theory shows that the mean rate of decomposition for molecules of excitation energy equal to the activation energy (that is to the difference between dissociative and molecular ionization threshold) for the formation of the first fragment ion, is quite large: $\sim 10^7$ s^{-1} for $Fe(CO)_5$ and $\sim 10^{11}$ s^{-1} for $Ni(CO)_4$ [21]. Very little if any kinetic shift [22] is therefore to be expected for the formation of $Fe(CO)_4^+$ and $Ni(CO)_3^+$ ions. Considering that the fragmenting ion becomes smaller and smaller with the fragmentation, the kinetic shift for the formation of the naked metal ions is expected to be no more than few hundredths of an electron volt. Actually the kinetic energy of the fragments corresponds to a temperature between 0 and 298 K. So the difference between calculated and experimental values is partially ascribed to translational energy ($\leqslant 0.2$ eV) and partially to internal excitation of the fragments. From these considerations an uncertainty of about 0.1 eV is estimated for all the fragmentation processes.

Average Bond Energies. From the threshold energies of Fe$^+$ from $Fe(CO)_5$, and the ionization energies of atomic iron and of $Fe(CO)_5$, it is possible to obtain the average bond dissociation energies for the neutral molecule $\overline{D}\ [Fe - (CO)_5] = 1.25 \pm 0.03$ eV, and for the molecular ion $\overline{D}$

$$[Fe - (CO)_5^+] = 1.23 \pm 0.03 \text{ eV}.$$

The first value must be compared with 1.20 eV from thermochemical data [21] and with 1.24 eV as calculated from the heats of formation of $Fe(CO)_5$, Fe and CO. These data suggest that the first ionization results by removing the electron from a virtually non-bonding or weakly bonding molecular orbital with a prevailing metal character. This agrees with the nature of the last occupied molecular orbital as calculated for the metal hexacarbonyls [24].

$Ni(CO)_4^+$. A typical photoionization field curve for the $Ni(CO)_4^+$ ion is shown in figures 3 and 4. The onset occurs at $1490 \pm 1 Å$ $(8.32 \pm 0.01 eV)$. This value is to be compared with the previous photoionization value of 8.28 eV [10]. As discussed for the $Fe(CO)_5^+$ ion, the $Ni(CO)_4^+$ ion also is likely formed by $0'-0''$ (or $1'-1''$, etc.) transitions. From the threshold value and the heat of formation of $Ni(CO)_4$ $(-144.10$ kcal mol$^{-1})$ [15] the ionic heat of formation,

$$\Delta Hf°[Ni(CO)_4^+] = 47.8 \pm 0.5 \text{ kcal mol}^{-1}$$

is obtained. Below 1450Å, the curve shows many autoionization peaks every $0.02-0.03$ eV, which compose broad maxima between 1450 and 1350Å and between 1310 and 1060Å. From the latter wavelength to 600Å, the curve is constant or slowly decreases in intensity.

$Ni(CO)_3^+$. The onset of the $Ni(CO)_3^+$ ion (see figs. 3 and 4) shows weak autoionization levels peaking at 1413, 1410, 1407, 1403, 1397, 1394, 1390, and 1388Å. These energies and the shape of the curve are the same as those of the molecular ion in the corresponding region. This again suggests that the $Ni(CO)_3^+$ ion is coming from the molecular ion and not from a $Ni(CO)_3$

radical formed by decomposition. The formation process of this ion at this energy seems to be:

(a) $Ni(CO)_4 + h\nu \rightarrow Ni(CO)_4^*$

(b) $Ni(CO)_4^* \rightarrow Ni(CO)_4^{+*} + e$

(c) $Ni(CO)_4^{+*} \rightarrow Ni(CO)_3^+ + CO$
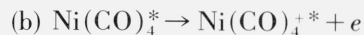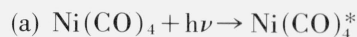
Process (a) and (b) refer to the autoionization of the molecule. Process (c) is ascribed to predissociating levels of the molecule ion leading to the $Ni(CO)_3^+$ ion. If this is true, the threshold of the $Ni(CO)_3^+$ ion is not affected by the thermal energy present in the neutral molecule. The thermal energy if present would have obscured the details of the curve structure. From the threshold value of $1414 \pm 1Å$ (8.77 eV), and the heats of formation of $Ni(CO)_4$ and CO,

$$\Delta Hf°[Ni(CO)_3^+] = 82.6 \text{ kcal mol}^{-1}$$

is calculated.

$Ni(CO)_2^+$. The steplike, very weak onset for $Ni(CO)_2^+$ ion occurs at $1228 \pm 1Å(10.10$ eV) (see fig. 4) resulting in a heat of formation, $\Delta Hf°[Ni(CO)_2^+] = 141.7 \pm 2$ kcal mol^{-1}. The curve shows a number of autoionization levels in the initial part, and a broad maximum between 985 and 895Å. From the latter energy to 600Å, the $Ni(CO)_3^+$ and $Ni(CO)_2^+$ curves are very similar.

$NiCO^+$. From the threshold value of 1064 ± 1 Å (11.65 eV) the heat of formation $\Delta Hf°[NiCO^+] = 203.8$ kcal mol^{-1} is calculated. The curve, shown in figure 4, exhibits the expected tail on the low energy side.

Ni^+. The Ni^+ ion curve starts with some weak autoionization peaks (see fig. 4). The shape of the curve at
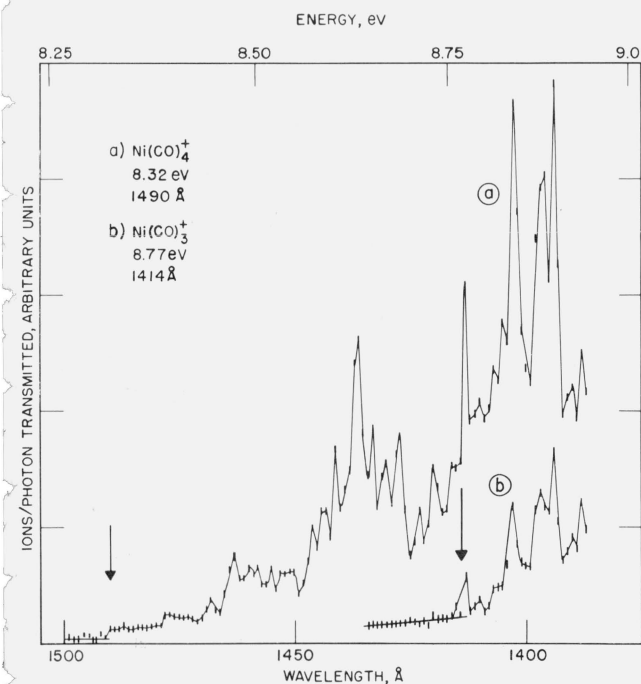

FIGURE 3. *Photionization-yield curves from onset to 1380Å for $Ni(CO)_4^+$ and $Ni(CO)_3^+$ ions from nickel tetracarbonyl.*
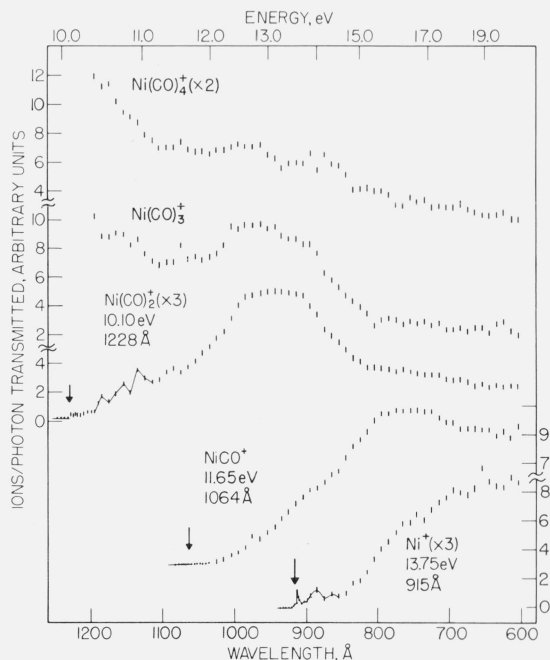

FIGURE 4. *Photoionization-yield curves from 1200 to 600Å for molecule and fragment ions of nickel tetracarbonyl.*

237

the onset, and the absence of a low energy tail suggest that the Ni^+ ion is not formed by a cascade process, but directly from the molecule ion. The onset is at 915 ± 1 Å (13.55 eV). Considering the thermal energy the neutral molecule possesses at 298 K (0.2 eV as calculated from ir frequencies [25] the threshold value might become 13.75 eV. From this value $\Delta Hf°(Ni^+) = 278.7$ kcal mol^{-1} is obtained.

From heats of formation $(\Delta Hf°(Ni) = 102.7$ kcal mol^{-1} (19), $\Delta Hf_0°$ $Ni(CO)_4 = -144.877$ kcal mol^{-1} [15] and from $I(Ni) = 7.63$ eV [20], the theoretical threshold for the Ni^+ ion is 13.82 eV at 298 K and 13.63 eV at 0 K. As for Fe^+ ion the kinetic shift involved in the production of this ion is very small. The increase of the translational and rotational degrees of freedom due to the fragmentation, could account for the difference between calculated (at 0 K) and experimental threshold value. Again the data show that the fragments possess kinetic energy corresponding to a temperature between 0 and 298 K. From the agreement between experimental and calculated threshold value, an error of about 0.1 eV is estimated for the fragmentation processes.

Average Bond Energy. The average bond dissociation energy for the neutral molecule and for the molecule ion (obtained as for the iron-carbonyl) are $\bar{D}[Ni\text{-}(CO)_4] = 1.53 \pm 0.03$ eV and $\bar{D}[Ni\text{-}(CO)_4^+] = 1.36 \pm 0.03$ eV respectively. The first value should be compared with 1.53 eV obtained from the thermochemical bond energy [26] and from the heats of formation of $Ni(CO)_4$, Ni and CO. The first ionization results from removing the electron from a partially bonding molecular orbital with prevailing metal character, in agreement with a calculated molecular orbital energy level diagram [27].

4. Conclusion

In electron impact experiments, ions formed by successive decompositions show a weak long tail on the low energy side. Due to the distribution of thermal energy of the electrons ejected from a hot filament, the threshold value determination is difficult for these ions by electron impact technique. For this reason, the bond energies and the heats of formation for the metal ions calculated from data obtained by electron impact [5–9] disagree with those obtained by thermochemical methods. The better resolution obtained by photon impact and the different threshold law allow one to obtain more accurate data. In fact bond energies and $\Delta Hf°(M^+)$ obtained by photon impact agree well with the thermochemical values.

The curves obtained by photon impact show several peaks assigned to autoionization processes previously not reported. Often the features of the $M(CO)_n^+$ ion curve are very similar to that of $M(CO)_{n+1}^+$ ion curve. Likely this fact can be ascribed to the formation of

the lower mass ion from that with one more CO ligand, even if metastable ions are not observed to confirm the fragmentation paths. The relative abundances of the ions differ from the values obtained by electron impact as discussed.

---

5. References

[1] Bruce, M. I., Advan. Organomet. Chem., **6**, 273 (1968).
[2] Chambers, D. B., Glockling, F., and Light, J. R. C., Quart. Rev., **22**, 317 (1968).
[3] Distefano, G., Innorta, G., Pignataro, S., and Foffani, A., J. Organomet. Chem., **14**, 165 (1968).
[4] Innorta, G., Distefano, G., and Pignataro, S., Intern. J. of Mass Spectrometry and Ion Phys., **1**, 435 (1968).
[5] Winters, R. E., and Kiser, R. W., Inorg. Chem., **3**, 699 (1964).
[6] Foffani, A., Pignataro, S., Cantone, B., and Grasso, F., Z. Physik. Chem. (Frankfurt), **45**, 79 (1965).
[7] Bidinosti, D. R., and McIntyre, N. S., Can. J. Chem., **45**, 641 (1967).
[8] Junk, G. A., and Svec, H. J., Z. Naturforsch. **23b**, 1 (1968).
[9] Schildcrout, S. M., Pressley, G. A., Jr., and Stafford, F. E., J. Am. Chem. Soc., **89**, 1617 (1967).
[10] Vilesov, F. I., and Kurbatov, B. L., Doklady Akad. Nauk. SSSR, **140**, 1364 (1961).
[11] Dibeler, V. H., and Reese, R. M., J. Res. Nat. Bur. Stand. (U.S.) NBS, **68A**, 409 (Phys. and Chem.), No. 4 (July–Aug. 1964).
[12] Dibeler, V. H., and Walker, J. A., J. Opt. Soc. Am., **57**, 1007 (1967).
[13] Pignataro, S., and Lossing, F. P., J. Organomet. Chem., **11**, 571 (1968).
[14] Day, J. P., Pearson, R. G., and Basolo, F., J. Am. Chem. Soc., **90**, 6933 (1968).
[15] Wagman, D. D., and Evans, W. H., private communication.
[16] Wagman, D. D., Evans, W. H., Parker, V. B., Halow, I., Bailey, S. M., and Schumm, R. H., Selected Values of Chemical Thermodynamic Properties, Nat. Bur. Stand. (U.S.), Tech. Note 270–3 (1968).
[17] Edgell, W. F., Wilson, W. E., and Summit, R., Spectrochimica Acta, **19**, 863 (1963).
[18] Chupka, W. A., and Russell, M. E., J. Chem. Phys., **48**, 1527 (1968).
[19] J.A.N.A.F. Thermochemical Tables, The Dow Chemical Co., Midland, Michigan, PB 168 370(1965), 370–1(1966), 370–2 (1967).
[20] Moore, C. E., Atomic Energy Levels, Nat. Bur. Stand. (U.S.), Circ. 467 (1968).
[21] Rosenstock, H. M., and Krauss, M., Adv. Mass Spectrometry, Vol. 2, and references (Pergaman Press, New York, 1962).
[22] Steiner, B., Giese, C. F., and Inghram, M. G., J. Chem. Phys., **34**, 189 (1961).
[23] Cotton, F. A., Fischer, A. K., and Wilkinson, G., J. Am. Chem. Soc., **81**, 800 (1956).
[24] Beach, N. A., and Gray, H. B., J. Am. Chem. Soc., **90**, 5713 (1968).
[25] Jones, L. H., McDowell, R. S., and Goldblatt, M., J. Chem. Phys., **48**, 2663 (1963).
[26] Fischer, A. K., Cotton, F. A., and Wilkinson, G., J. Am. Chem. Soc., **79**, 2044 (1957).
[27] Schreiner, A. F., and Brown, T. L., J. Am. Chem. Soc., **90**, 3366 (1968).

(Paper 74A2–595)

Symposium on Electronic Density of States

Electronic Density of States was the subject of the 3d Materials Research Symposium, sponsored by, and held at the National Bureau of Standards, Gaithersburg, Md. on November 3–6, 1969. Attention was focussed on the correlation of various experimental and theoretical techniques such as optical methods; photoelectron, soft x-ray, and ion neutralization spectroscopy; specific heat; Knight shift; and magnetic susceptibility. Band theory and many-body effects, as they relate to the electronic density of states, were included.

Approximately 100 papers were presented at these sessions, including 16 invited presentations. Six of these invited papers are being published in this issue of the Journal; the remaining ten will appear in succeeding issues. All of the papers presented at the Symposium will be published by the National Bureau of Standards as Special Publication 323 which will appear later this year.